JJMIE

Volume 18, Number 4, December. 2024
ISSN 1995-6665
Pages 737- 752
https://doi.org/10.59038/jjmie/180409
Editor-in-Chief: Prof. Ali M. Jawarneh

Jordan Journal of Mechanical and Industrial Engineering

Improvement of Wear Rate Properties of a Brown Pumice and Coal Ash Particulates Reinforced Aluminum Composite for Automobile Brake Manufacturing, Through Optimization and Modelling

Tanimu Kogi IBRAHIM[a *], Julius THADDAEUS[a], Caleb Abiodun POPOOLA[c], Ibrahim ILIYASU[b], Abdulmumin Akoredeley ALABI[b]

[a] *Mechanical Engineering Department, Faculty of Engineering, Federal University Wukari, Nigeria*
[b] *Mechanical Engineering Department, Ahmadu Bello University, Zaria, Nigeria*
[c] *Chemical Engineering Department, Faculty of Engineering, Federal University Wukari, Nigeria*.

Received 5 Jun 2024 *Accepted 13 Aug 2024*

Abstract

This research optimized the specific wear rate property of a hybrid reinforced aluminum metal matrix composite for brake disc manufacturing. Pumice and carbonated particulates were produced and characterized using XRF, XRD, and TGA/DTA. The Taguchi design of the experiment was utilized to develop experimental runs for casting the aluminum, brown pumice, and coal ash hybrid composites and the control using double-stir gravity casting technique. The specific wear rate of the material was extensively studied via Taguchi optimization techniques and regression analysis. The XRD shows that the predominant phases in pumice particles are silica, anorthite, and albite, whereas silica, graphite, and muscovite were detected in coal ash particulates. The AA6061 (aluminum alloy) XRF analysis revealed the presence of aluminum (97.74%), silicon (0.61%), and magnesium (0.82%) as the predominant elements. In the pumice particles, the major constituents were 20.59% silicon, 12.35% iron, 8.57% calcium, and 7.91% aluminum, while in coal ash particles, the major elements were 22.14% silicon, 8.91% iron, and 7.56% aluminum. The thermogravimetric results revealed that the aluminum alloy, brown pumice, and coal ash used could endure high temperatures of up to 264.08, 724 °C, and 606.61°C, respectively, before deterioration. The best specific wear capacity of 2.4002 and 2.5 mm^3/Nm at 10 % brown pumice, 5 % coal ash, 500 rpm stirrer speed, 850 °C pouring temperature, and 20 minutes stirring duration for predicted and experimental were obtained. The mathematical model developed using regression analysis shows a high level of predictability of 98.61%, 93.16%, and 80.74% as R-square (R^2), R-square (adj), and R-square (pred) values.

Keywords: Aluminum Hybrid Composite; Taguchi Optimization; Regression Analysis; Brake Disc; Specific wear rate.

1. Introduction

In the realm of automotive engineering, there is a perpetual quest for safer, more efficient, and longer-lasting brake systems [20, 25]. As vehicles evolve, so also the materials and technologies that underpin their crucial components, including brake systems [39],[81]. Brake systems are integral to automotive safety, providing the means to decelerate or stop vehicles efficiently and reliably [68], [73]. Traditionally, brake components have been manufactured from materials such as cast iron, which offer commendable performance but also exhibit drawbacks such as high weight and susceptibility to wear. However, there has been a recent shift towards adopting composite materials for brake applications. Composites, by their nature, allow for the combination of different materials to achieve desired properties, thereby offering a pathway to overcoming the limitations of conventional materials (cast iron, steel, and aluminum) [5, 10, 38]. Researchers are exploring alternative materials like Aluminum Matrix Composites (AMCs) reinforced with various particulates to address this issue [9], [12],[15],[35], [41],[84].

Aluminum Matrix Composites (AMCs) are lightweight materials that exhibit high performance and are aluminum-based in nature [12], [87]. The reinforcements in these aluminum-based composites may be whiskers or particles or continuous or discontinuous fibers. Sometimes, these reinforcements may be up to 70% content of the composites [26], [54],[18]. The behavior or properties of the aluminum-based composites may be easily fine-tuned to meet the needs of different industrial applications ranging from high strength, anti-corrosion, high wear resistance, and high fatigue strength [64]. Furthermore, these property

* Corresponding author e-mail: terrytanimu@yahoo.com.

alterations may involve simple processes like changes in the processing methods, reinforcement type or quantity, and processing parameters. Therefore, this implies that aluminum matrix composites are produced using various methods. Considerable attention has been directed towards understanding how different reinforcements affect the overall behavior of aluminum matrix composites [45], [66], [52],[55], [85], [16]. Furthermore, the mechanical, thermo-mechanical, tribological, and chemical attributes of these reinforced aluminum metal matrix composites have been extensively studied with exciting and valuable results,[24], [29], [11],[44], [46], [56], [60], [68]-[73].

In recent years, exploring novel materials and composite formulations has emerged as a promising avenue for enhancing wear resistance in automobile brake applications. One of such intriguing direction involves the utilization of brown pumice and coal ash particulates as reinforcements in aluminum matrix composites [68]-[73]. Brown pumice and coal are abundant under-utilized solid minerals that offer a sustainable and economically viable solution to this challenge. Their unique properties, including their lightweight nature, high-temperature resistance, and inherent abrasion resistance, make them attractive candidates for integration into aluminum-based composites tailored for brake applications [68], [83].

Brown pumice, a lightweight volcanic rock characterized by its porous structure and abrasion resistance, offers the potential to enhance the composite's wear resistance while contributing to overall weight reduction. Coal ash is a unique material produced when coal is heated in an oven between temperatures 500 and 1300 °C in an air-deprived environment. It is composed of high amounts of graphite, SiO_2, Al_2O_3, and Fe_2O_3, making it an excellent candidate for reinforcement in composite materials [70]-[73]. Coal ash particulates possess desirable characteristics such as high-temperature stability, chemical inertness, and mechanical strength. These properties make coal ash an attractive reinforcement for aluminum matrix composites intended for high-temperature applications such as automotive brakes [43], [48].

The attributes of composites (metal matrix) are affected not only by the type, size, geometry, and reinforcements volume but also by the manufacturing route used to produce them. Stir casting is the most often employed production route for composites (metal matrix), offering an economical method of production [77]. This process involves dispersing reinforcing material particles into molten aluminum using mechanical stirring [33]. However, the conventional stir-casting process has its own disadvantages, such as particle segregation due to reinforcing particles settling during solidification. To address these issues, a two-step mixing process, also referred to as double stir casting, has been developed. In this technique, the matrix is heated beyond its liquidus point and then allowed to cool to a temperature range between the solidus and liquidus, achieving a semisolid state. Preheated reinforcements are then introduced and thoroughly blended through vigorous mixing. The resulting mixture is reheated until it reaches an entirely liquid state and stirs vigorously once more [65]. This approach results in a more homogeneous microstructure than traditional stirring, as it shatters a layer of gases around the particle surface, leading to better wetting of the molten metal and reinforcement particulates [65], [32]. Studies have shown that this method effectively produces MMCs with improved microstructural homogeneity [65],[36].

The casting process parameters significantly affect the cast product's quality and properties. These parameters play a crucial role in the reaction synthesis that occurs during composite melt processing and need to be carefully monitored and controlled. To achieve a uniformly distributed reinforcement throughout the microstructure, the reinforcement distribution, porosity, wettability problems, and reaction viscosity should be addressed by selecting and monitoring the casting process parameters. Researchers have employed various mechanical stirring process parameters in the production of aluminum matrix composites to optimize the composite's ultimate microstructure [58], [68]-[73], [62], [86]. An investigation was conducted to determine how different process parameters, such as pouring temperature, stirrer speed, and stirring duration, in addition to reinforcements' volume fraction, influence the properties of composites. Many researchers have deployed different optimization techniques such as response surface methodology [17], [37], [63],[74], [82], Taguchi [57], [67], [68], [70]-[73] and fussy logic to optimize process parameters of various processes. But out of these techniques Taguchi method has been preferred compares to others due to its cost effectiveness and been robust.

The study aims to develop and optimize cost-effective and high-performance materials hybrid composites for brake disc applications. The study employed the Taguchi optimization technique, a robust statistical method that optimizes process parameters and enhances product quality, to determine the optimal volume percentage of reinforcements and process parameters for stir casting. Recent research has improved the Taguchi optimization technique's output response by considering input factors that influence the performance metrics of the method [34], [69], [14], [67]. This study presents several novel contributions in the development of aluminum composites reinforced with pumice and coal ash for brake disc applications. Firstly, it introduces cost-effective and sustainable alternatives to traditional synthetic reinforcements by utilizing pumice and carbonated coal which are readily available. This not only reduces production costs but also aligns with environmental sustainability goals by repurposing these materials. Secondly, the application of the Taguchi methodology provides a systematic and efficient approach to design experimental runs and optimize process parameters. This ensures reliable manufacturing processes and enhances the overall performance of the hybrid composites. Thirdly, the use of regression analysis offers a quantitative assessment of how each process parameter impacts the tensile strength of the composites. This analytical approach yields crucial insights into optimizing reinforcement percentages and processing conditions to achieve desired mechanical properties essential for brake disc reliability and durability. In essence, the study integrates innovative material selection, advanced experimental design, and rigorous analysis techniques to advance both the cost-effectiveness and performance optimization of brake disc materials.

2. Materials and Methods

2.1. Materials

The materials used to produce the Al-BP-CA hybrid composite are coal, brown pumice (BP), and aluminum alloy (AA6061). The coal was acquired from a coal mine in Effeche-Akpalli, Benue State, Nigeria. The brown pumice was also extracted from an underground mining site in Biu, Borno State, Nigeria. The physical properties of aluminum, pumice and coal ash are shown in Table 1.

Table 1. Physical properties of Aluminum, Pumice, and Coal Ash

Property	Aluminum Alloy AA6061	Pumice	Coal Ash Particles
Density (g/cm³)	2.70	0.25 - 1.5	~1.3 - 1.7
Melting Point (°C)	582 - 652	1,100 - 1,500	~1400 - 1,600
Thermal Conductivity (W/m·K)	167	~0.1 - 0.5	~0.15 - 0.3
Specific Heat Capacity (J/g·K)	0.896	~0.84-1.1	~1.0

2.2. Brown Pumice Particulates Production Process

The brown pumice was washed and dried for 48 hours at 100 °C to remove filth and moisture. Respectively. The aggregated were pulverized with a laboratory mortar and pestle before being processed into powders using a ball milling machine. This production technique is consistent with the research results of Ibrahim *et al.* [70] and Jayakrishnan andJayakrishnan[49]. The brown pumice particulates were further sieved per BSI 377:1990 standard into three different particle sizes (90 μm, 56 μm, and 25 μm).

2.3. Production of Coal Ash Particulates

The coals were washed and dried for 48 hours at 100 °C to remove moisture and filth before pulverizing them using a jaw crusher. The pulverized coals were put in a crucible made of graphite and subjected to heating to about 1100 °C in an electrical furnace without any air for 8 hours. After being normalized in the oven, it was processed into powders using a ball milling machine. This method is supported by research by Hassan and Gomes [42] and Sharma *et al.*[18]. The generated carbonized coal underwent further sieving per BSI 377:1990 standard to produce carbonized coal ash particles 25, 53, and 90 μm particle size.

2.4. Experimental Design

Taguchi's design methodology was used to plan experimental runs. In this study, five factors: brown pumice particulate (BP) (wt%), coal ash particles (CA) (wt%), stirrer speed (SP) (rpm), stirring duration (SD) (min), pouring temperature (°C), and their four different levels were considered to be studied as shown in Table 2. The reinforcement, stirrer speed, pouring temperature, and stirring duration limits and levels were selected, referencing previous studies conducted by Adebisi and Ndaliman [3] and Ibrahim et al. [69]. Minitab 19 software was employed to create the L_{16} orthogonal array for the 16 experimental trials, shown in Table 3.

Table 2. Reinforcements and Stir Casting Process Parameters Factors and Levels

S/N	Processing Factors	Unit	Factors Designation	Level			
				1	**2**	**3**	**4**
1	Brown Pumice	Wt%	BP	2.5	5	7.5	10
2	coal Ash	Wt%	CA	2.5	5	7.5	10
3	Stirrer Speed	rpm	SS	200	300	400	500
4	Pouring Temperature	°C	TP	700	750	800	850
5	Stirring Duration	min	SD	5	10	15	20

Table 3. L_{16} Orthogonal Array for Production of Hybrid Composite

Experimental Run	Factors				
	BP (vol%)	**CA (vol%)**	**SS (rpm)**	**TP (ºC)**	**SD (min)**
1	2.5	2.5	200	700	5
2	2.5	5	300	750	10
3	2.5	7.5	400	800	15
4	2.5	10	500	850	20
5	5	2.5	300	800	20
6	5	5	200	850	15
7	5	7.5	500	700	10
8	5	10	400	750	5
9	7.5	2.5	400	850	10
10	7.5	5	500	800	5
11	7.5	7.5	200	750	20
12	7.5	10	300	700	15
13	10	2.5	500	750	15
14	10	5	400	700	20
15	10	7.5	300	850	5
16	10	10	200	800	10

2.5. Al-BP-CA Hybrid Composites Fabrication

The composites were produced using a two-stepstir casting procedure described by Ikubanni*et al.* [51] and Adedirani*et al.*[4] using a bottom pouring stir casting machine (model- L2: 700-2000g, brand: SwamEquip) at SwamEquip, Chennai, India.

Prior to the casting process, the brown pumice and coal ash particles underwent a preheating treatment for 2 hrs at 500 °C per the recommendations of previous investigations by Kumar *et al.*[13] and Adebisi*et al.*[1] to oxidize and calcine the particle surfaces. Subsequently, the aluminum alloys (AA6061) were fed into the furnace and heated to 800 °C to guarantee thorough alloy melting. Before incorporating the preheated reinforcements, the surface dross was initially eliminated. Afterward, 0.01% NaCl (to eliminate gases) and 1% magnesium powders (to enhance wettability) were introduced into the molten aluminum [78]. The liquid alloy undergoes controlled cooling within the furnace until it reached a temperature of 610 °C, transitioning into a semisolid state. Subsequently,an automated stainless-steel stirrer coated with a protective layer was lowered into the melted aluminum alloy in the furnace to initiate stirring to form a vortex within the melt. The preheated particulate materials were introduced gradually into the molten slurry at a steady flow rate of 5 grams per minute. Subsequently, the mixture was reheated to the prescribed pouring temperature, stirrer speed, and time as specified in the experimental run of the design plan. The mold was heated to around 450 °C before pouring the slurry into it [13].

For each of the experimental trials, this methodology was adhered to, with careful consideration of the process parameters and the reinforcement percentage as recommended in the design plan [2]. A control (without reinforcement) was also produced to compare the effects of the reinforcement. The cast hybrid composites are shown in Figure 1 (b).

2.6. Characterization of the Constituents

Both matrix (aluminum AA6061) and reinforcement (brown pumice and coal ash) were characterized using XRF, SEM-EDS, XRD, and TGA/DTA to determine their chemical composition, morphology, crystalline structure, and thermal stability [73], [75], [86].

2.7. Specific wear rate

This test complies with ASTM G 99-17 standard [40, 59]utilizing a pin-on-disc tribometer computer integrated wear & friction monitor (model:TR-201CL Manufacturer: Ducom) [8], [27]. Wear and COF tests were conducted by exerting a force of 8 Newton at a constant speed of 10 cm/s and 50 m sliding distance.

In this process, an electronic weighing machine with a precision of 0.01g was used to measure the sample's initial and final weights. Equation 1 was then applied to compute the specific wear rate [19].

$$SWR = \frac{\Delta M}{\rho DF} \quad (1)$$

Where SWR is the specific wear rate (mm^3/Nm), ΔM is the mass loss (g), F (N) denotes applied force, ρ (g/cm^3) is the density, and D is the sliding distance in meters. All experiments were conducted at 29 °C and 55% temperature and relative humidity, respectively [51]. Figure 1 (a) shows the experimental setup for the wear test while Figure 1 (c) and (d) samples for wear test before and after respectively

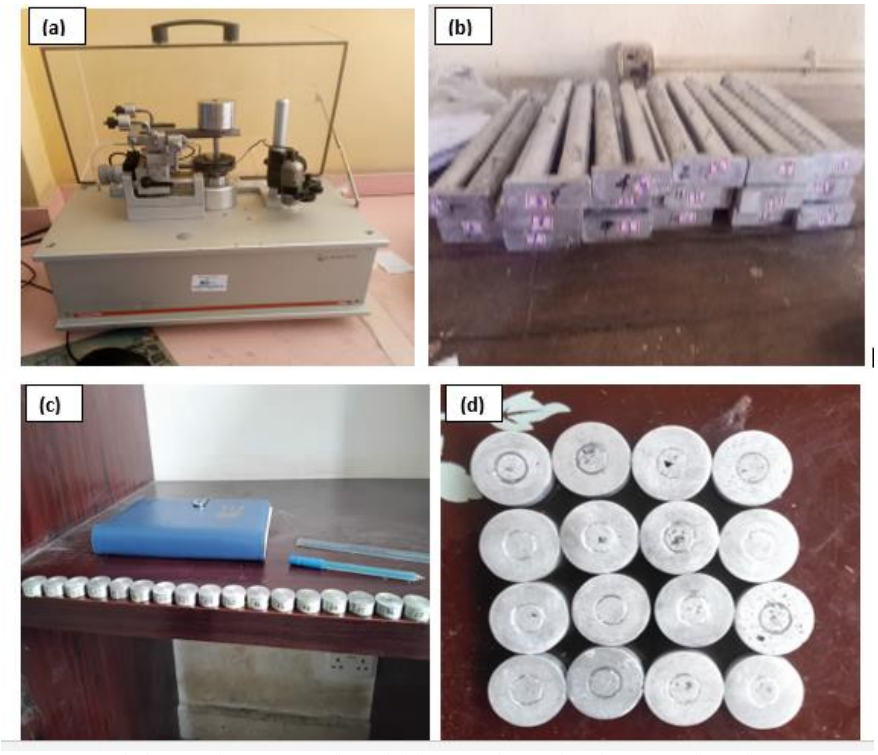

Figure. 1. (a) Ducom Wear & Friction Monitor TR-201; (b) Hybrid Composite Produced; (c) Samples Before Wear Test; (d) Samples After Wear Test

2.8. Statistical Analysis and Optimization

The Al-BP-CA composites' specific wear rates were analyzed experimentally using Taguchi optimization [68-73] and ANOVA [61] with the aid of Minitab software (21.4.2). The study employed a "larger-the-better" objective function in Taguchi optimization to optimize the process parameters that can give us the best composite's specific wear rate[73], [23].

Confidence interval (CI)

The confidence interval for this analysis was evaluated using Equation 2 [70].

$$C.I. = \sqrt{f_{\propto(1,d_e)} v_e \left(\frac{1}{m} + \frac{1}{n}\right)} \quad (2)$$

Where $f_{\propto(1,d_e)}$ is the F Distribution Critical Values (α=0.05 significance level) between 1 and d_e(which is the degree of freedom of error), gotten from statistical tables, v_e is the variance (mean square) of error, which are obtained from the analysis of variance. N is the number of effective replications. M was evaluated using Equation 3 [73].

$$M = \frac{Total number of experiment}{1 + degree of freedom of control factors} \quad (3)$$

3. Results and Discussion

3.1. Constituting Materials' XRF Results

The Constituents (aluminum alloy (AA6061), brown pumice, and coal ash particles) of the Al-BP-CA hybrid composites were examined via an XRF analyzer. Tables 4 and 5 present the results of the investigation. The XRF results of the aluminum alloy, as displayed in Table 3, indicate that aluminum, silicon, and magnesium are the predominant constituents. This finding corroborates the findings of Kareem *et al.*[11], Ibrahim *et al.*[71] and Ibrahim *et al.*[68].

Table 5 shows the XRF results of the coal ash and pumice particulates. The analysis verified that coal particle ash predominantly consisted of Si, Al, Fe, Ti, and Ca. The major constituents of brown pumice particulates were Si, Fe, Al, Ca, K, and Ti. These outcomes are similar to investigations by Ibrahim *et al.*[70], Ibrahim *et al.*[72] and Dagwa and Adama [31]. The presence of these elements indicates that brown pumice and coal ash particulates have the potential to serve as effective particulate reinforcements in metal matrices given their chemical composition, which shares similarities with certain agricultural and industrial residue (bagasse, Coconut fiber ash, and Banana fibers ash, fly ash, bottom ash, and red mud) [22],[28].

3.2. Constituting Materials' X-ray Powder Diffraction

Based on the XRD patterns of brown particles (BP) displayed in Figure 2, it is evident that the patterns include peaks corresponding to an amorphous quartz (SiO_2) material, along with specific crystalline phases of anorthite (Ca $Al_2(SiO_4)_2$) and albite ($NaAlSi_3O_8$). These findings correlate with Ersoy*et al.*[24] and Pinarci and Kocak [32] findings. Upon matching the coal ash particles, distinct phases of SiO_2, graphite(C), and muscovite ($KAl_2(AlSi_3O_{10})(F,OH)_2$) were identified, as shown in Figure 1. This observation aligns with the research conducted by Ibrahim *et al.*[70] and Sahajwalla *et al.* [79], who identified some of these compounds in coal ash.

3.3. Thermogravimetric and derivatives of thermal analysis of aluminum alloy

The TGA-DTA curves in Figure 3 demonstrate a two-step weight loss for aluminum alloy when heated from 30 °C to 1000 °C in a nitrogen atmosphere. The TGA curve in the figure shows a significant drop until it is parallel to the temperature axis at approximately 513 °C.

The initial 1.16% weight loss occurs between a temperature of 83.29 and 264.08 °C, which can be linked to the evaporation of the absorbed surface moisture and some volatile matter. The major decompositions of the materials occur in one stage between the temperatures of 264.08 and 513 °C with a mass loss of 81.2%.

3.4. Thermogravimetric and derivatives of thermal analysis of brown pumice particulates

The TGA-DTA curves in Figure4 depict a two-step weight loss pattern for brown pumice particulateswhen exposed to a nitrogen gas atmosphere and heated within the temperature range of 30°C to 1000°C. The TGA curve in the figure demonstrates a substantial decline until it aligns parallel to the temperature axis around 957 °C.

Table 5. BP and CA Chemical Composition

S/n	Elements	Brown pumice (%)	Coal ash Particles (%)
1	O	42.267	46.52
2	Al	7.907	7.556
3	Si	20.594	22.141
4	P	0.288	0.000
5	S	0.074	4.415
6	Cl	0.718	1.721
7	K	4.212	1.130
8	Ca	8.574	2.667
9	Ti	2.140	3.500
10	V	0.084	0.140
11	Cr	0.008	0.170
12	Mn	0.198	0.268
13	Fe	12.348	8.910
14	Co	0.070	0.062
15	Ni	0.010	0.066
16	Cu	0.046	0.147
17	Zn	0.029	0.014
18	Zr	0.157	0.322
19	Nb	0.050	0.054
20	Mo	0.002	0.011
21	Ag	0.027	0.031
22	Ba	0.186	0.123
23	Ta	0.012	0.035

Table 4. Aluminum's XRF Results

Element	Al	Si	Fe	Cu	Mn	Mg	Zn	Cr	Ti	Ca	others
vol%	97.74	0.61	0.44	0.16	0.02	0.82	0.01	0.07	0.01	0.05	0.07

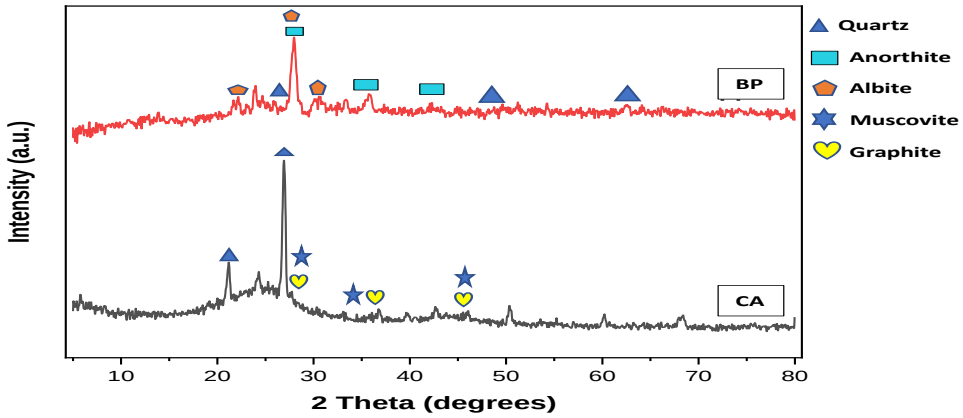

Figure 2. XRD Results of BP and CA particles

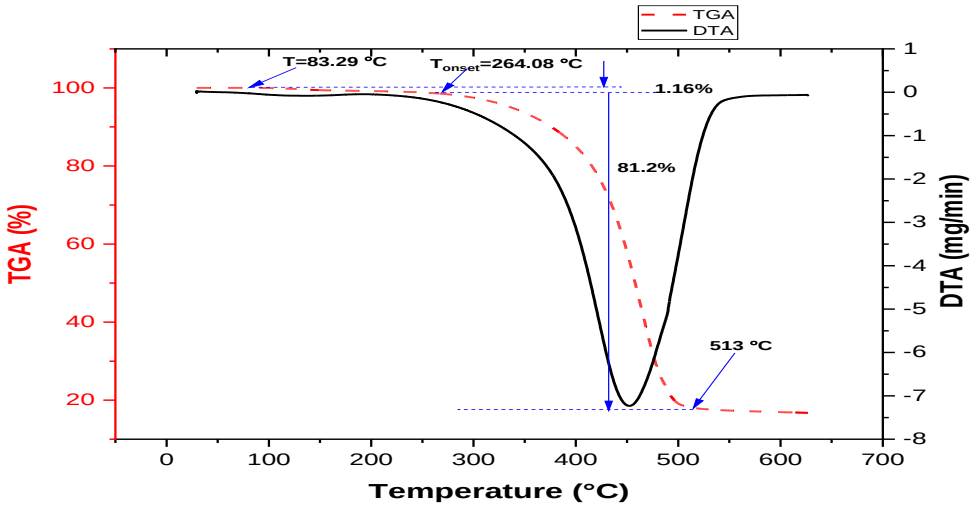

Figure 3. TGA-DTA curves of the Aluminum Alloy (AA6061)

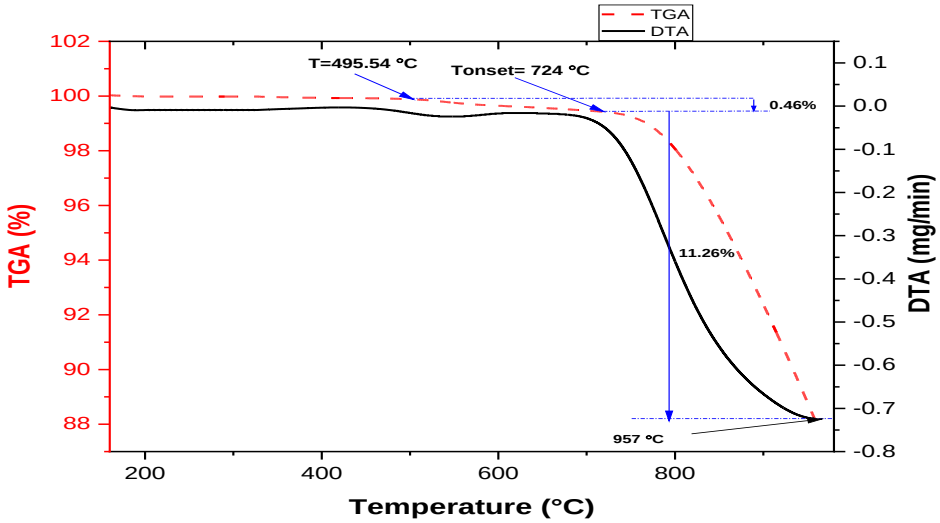

Figure 4. TGA-DTA curves of the Brown Pumice Particle

The initial 0.46% weight loss occurs between a temperature of 495.54 and 724 °C was observed, which can be linked to the evaporation of the absorbed surface moisture and some volatile matters. The major decompositions of the materials occur in one stage between 724 and 957 °C with a mass loss of 11.26%. The major decompositions in pumice can be accredited to the thermal decomposition of volatile substances such as sulfur dioxide (SO_2), carbon dioxide (CO_2), nitrogen, and various trace gases that may be present in the volcanic environment during the rock's formation. The lower mass loss in brown pumice particulates is owing to its high melting points (1343 °C) and the presence of TiO_2 (1843 °C) and SiO_2 (1710 °C), the major constituents, compared to the lower melting temperature of the aluminum alloy. This observation is similar to the work of Gencel [47].

3.5. Thermogravimetric and derivatives of thermal analysis of coal ash particulates

The TGA-DTG curves in Figure 5 demonstrate a three-step weight loss for coal ash particulateswhen exposed to a nitrogen gas atmosphere and heated within the temperature range of 30°C to 1000°C. The TGA curve in the figure shows a significant drop until it becomes parallel to the temperature axis at approximately 980.04 °C.

The initial 1.2% weight loss occurs between a temperature of 238.67 and 605.51 °C observed, which can be linked to the evaporation of the absorbed surface moisture and volatile matter. The major decompositions of coal ash particulates occur in two stages: in the temperature range of 605.51 °C to 840.52 °C, resulting in a mass reduction of 13.68%. Subsequently, the second phase occurred between 840 °C and 980.4 °C, with a mass loss of 24.38%. The first stage of major decomposition in coal ash particulates can be attributed to the volatile components such as water, hydrocarbons, or other gases trapped within the coal particles. The second stage might be due to the decomposition of carbonated minerals into oxides, which release carbon dioxide (CO_2) gas. The reduced mass loss in coal ash particulates is attributed to the elevated melting points of their primary constituents, TiO_2 and SiO_2 (1843°C and 1710°C, respectively), in comparison to the lower melting temperature of the aluminum alloy.

3.6. Specific wear rate (SWR) results of Al-BP-CA hybrid composite

Table 6 shows the results of a specific wear rate test performed on sixteen hybrid composites and a control sample, along with their signal-to-noise ratios. From the table, the specific wear rate of the as-cast aluminum alloy is greater than that of the 16-produced hybrid composite; this phenomenon may be ascribed to the inclusion of hard ceramic and graphite that are found in the coal ash and brown pumice reinforcements as indicated in the XRD analysis in Figure 2. This study agrees with the studies carried out by Aigbodion *and* Hassan[80], Apasi *et al.* [7], and Ashok-Kumar and Devaraju[53], who found that adding hard ceramic to the metal matrix composite increases its wear resistance.

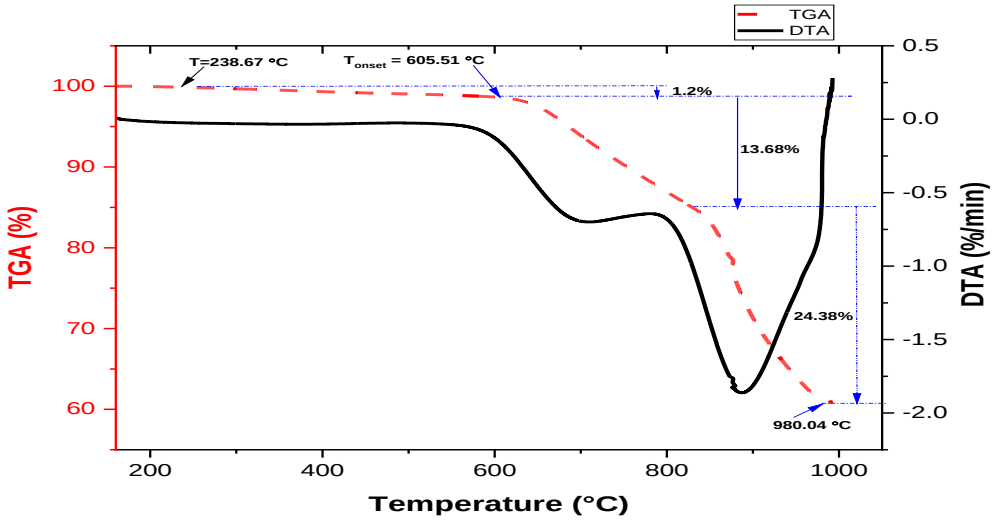

Figure 5. TGA-DTA curves of the coal ash particulates

Table 6. Specific Wear Rate Test Results and their Respective Signal to Noise Ratios

Runs	Factors					Specific Wear Rate	
(S/N)	BP (wt%)	CA (wt%)	SP (rpm)	PT (°C)	SD (min)	Mean x 10^{-6} (mm^3/Nm)	S/N ratio (dB)
1	2.5	2.5	200	700	5	4.90	-13.8
2	2.5	5	300	750	10	4.50	-13.06
3	2.5	7.5	400	800	15	3.90	-11.82
4	2.5	10	500	850	20	4.20	-12.47
5	5	2.5	300	800	20	4.40	-12.87
6	5	5	200	850	15	4.10	-12.26
7	5	7.5	500	700	10	4.30	-12.67
8	5	10	400	750	5	5.00	-13.98
9	7.5	2.5	400	850	10	3.10	-9.83
10	7.5	5	500	800	5	3.20	-10.1
11	7.5	7.5	200	750	20	3.80	-11.6
12	7.5	10	300	700	15	4.70	-13.44
13	10	2.5	500	750	15	3.10	-9.83
14	10	5	400	700	20	3.00	-9.54
15	10	7.5	300	850	5	3.30	-10.37
16	10	10	200	800	10	4.60	-13.26
Mean						**4.01**	**-11.93**
	Control (As Cast)					7.60	

3.7. Taguchi Optimization of Reinforcements Casting Process Parameters

The lower-the-better objective function was used to observe the optimum and the most influential parameters of stir casting process of aluminum hybrid composite.This analysis gave signal-to-noise ratios, main effect plots for the mean of the response, and that of signal-to-noise ratios, as presented in the discussions below;

3.7.1. Effect of reinforcement and stir casting process parameter on the specific wear rate

The impact of brown pumice particulates, coal ash particulates, stirrer speed, pouring temperature, and stirring duration on the specific wear rate is shown from Figure 5 to Figure 9.

3.7.1.1. Effect of pumice particulates on specific wear rate

Figure 6 displays the impact of brown pumice particulates on the specific wear rate of the composite produced. It shows that the specific wear rate increases as the brown pumice particulate content increases from 2.5 to 5 %; beyond this point, it shows a positive relationship between the wear rate and the brown pumice particulates' content (i.e., The wear rate demonstrates a decrease with a rise in the brown pumice particulate content). The decrease can be attributed to hard minerals (ceramics) in the pumice, such as quartz, anorthite, and albite. This finding aligns with similar observations reported in several studies, including those by VeeraVeeravalli *et al.*[56], Aigbodion and Hassan [80], Abdelkawy [6], and Apasi *et al*. [7]. The composite's best (optimum) wear rate from the analysis was 3.5 x 10^{-6}mm^3/Nm at a brown pumice particulate content of 10 %.

3.7.1.2. Effect of coal ash particulates on specific wear rate

Figure 7 indicates a reduced wear rate between the coal ash particulate content of 2.5% to 5.0%; beyond this point, the aluminum composite's wear rate increased. The decrease might be due to good wettability and even distribution of the coal ash particulates in the aluminum matrix. The lubricating nature of graphite within the coal might also contribute to the observed decrease. At the same time, the increase can be ascribed to the inadequate wettability and nonuniform distribution of the coal ash particulates in the matrix at a higher weight fraction. This result implies that the optimum composition of coal ash particulates for minimum wear rate is 5 %. These observations align with the work of Ashok-Kumar and Devaraju [53] and Prashant *et al.*[62]. From this analysis, the composite's best (optimum) wear rate was 3.7 x 10^{-6}mm^3/Nm at a brown pumice particulate content of 5 %.

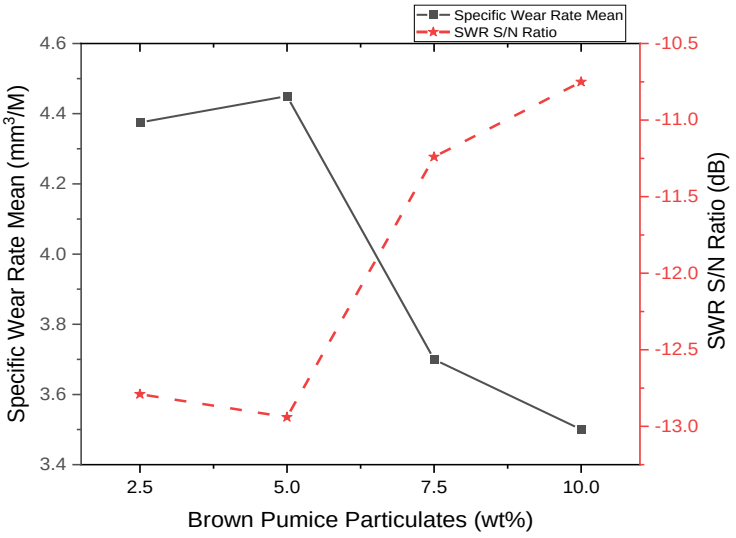

Figure 6. Variation of Brown pumice with Specific Wear Rate of the Aluminum Hybrid Composite

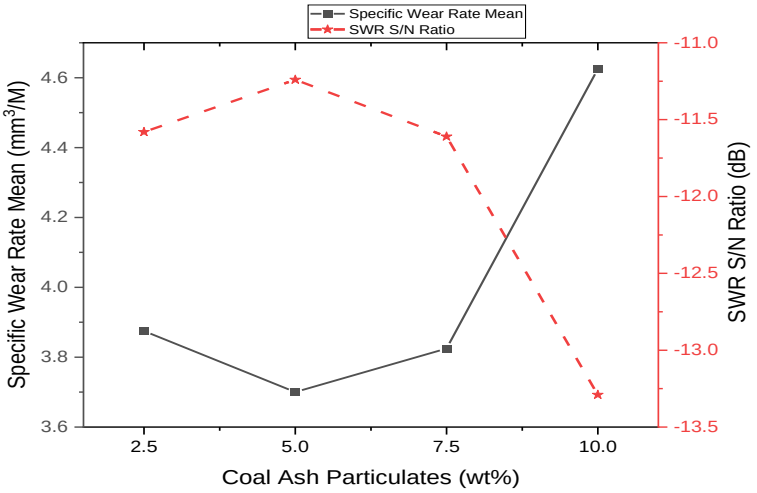

Figure 7. Variation of Coal Ashwith Specific Wear Rate of the Aluminum Hybrid Composite

3.7.1.3. Effect of stirrer speed on the specific wear rate

Figure 8 displays a general decrease in wear rate with increased stirrer speed; this phenomenon might be attributed to the proper mixing of the pumice and coal ash particulates in the aluminum alloy matrix. This finding suggests that elevating the stirrer speed generally leads to a better dispersion of the reinforcements throughout the matrix, thereby decreasing the material's wear rate. This outcome agrees with the findings reported by Sadi *et al.*[66] and Gupta *et al.* [43]. The optimum specific wear rate of 2.35 x 10^{-6} mm^3/Nm was observed to be the best at a stirrer speed of 500 rpm.

3.7.1.4. Effect of stirring temperature on specific wear rate

Figure 9 illustrates the positive impact of pouring temperature on the wear rate of the aluminum composite. It demonstrates that as the pouring temperature increases, the wear rate decreases. Specifically, the lowest (optimal) specific wear rate observed was 2.598 x 10^{-6} mm^3/Nm at a temperature of 850 ℃. The decrease can be attributed to the reduced viscosity and contact angle between the melted aluminum alloy, which enhances the distribution and wettability of the reinforcement in the matrix. This study is consistent with Hashim *et al*. [33], Sadi *et al*. [66], and Jayashree *et al*. [50].

3.7.1.5. Effect of stirring duration on the specific wear rate

As was observed in Figure 10, increasing the stirring duration reduces the specific wear rate of the reinforced aluminum composite; this is connected to the homogeneity of the reinforcements achieved with more stirring. The lowest (optimal)specific wear rate of 2.75 x 10^{-6} mm^3/Nm was observed at a stirring duration of 20 minutes. This result is similar to Malau *et al*. [76]; Sadi *et al*. [66]. The results of their study suggested that a longer stirring duration leads to a higher level of homogeneity in the distribution of reinforcements within the matrix. This, in turn, results in an increase in both the hardness and the wear rate resistance of the material

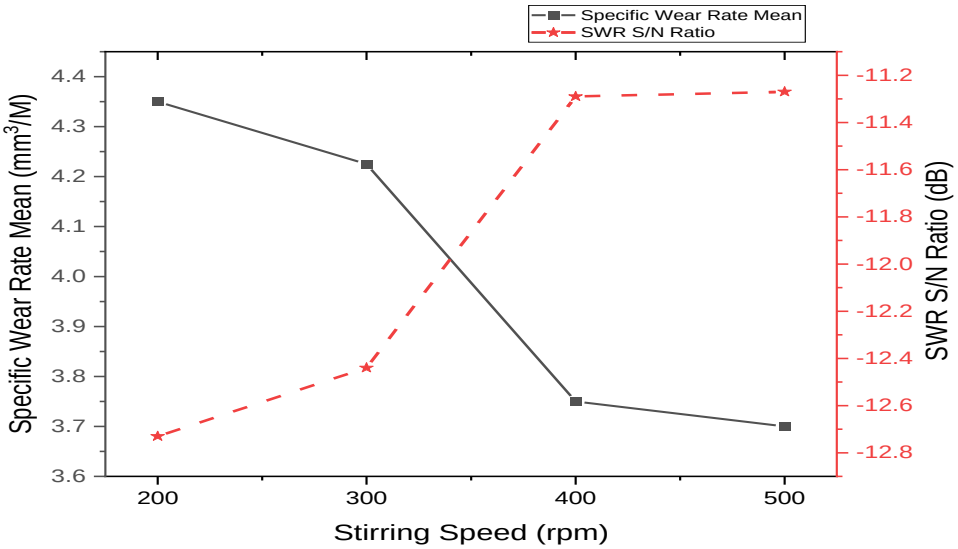

Figure 8. Variation of Stirrer Speed on the Specific Wear Rate of the Aluminum Hybrid Composite

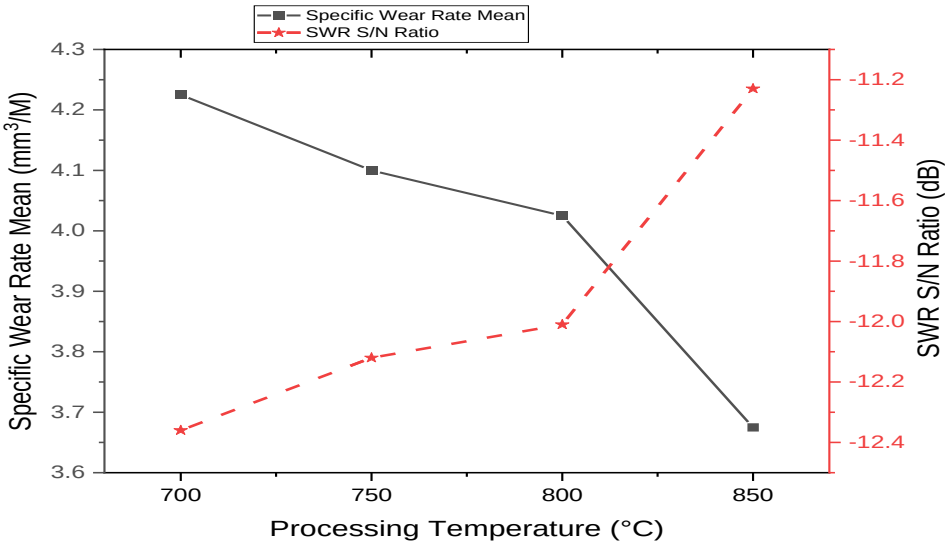

Figure 9. Variation of Pouring Temperaturewith Specific Wear Rate of the Aluminum Hybrid Composite.

3.8. Optimum combination for specific Wear rate

From Figure 6to Figure 10, the optimum reinforcements and process parameters of stir casting that gave the best specific wear rate are brown pumice particulate content (BP) at 10 %, coal ash particulates (CA) at 5 %, with a stirrer speed (SP) of 500 rpm, at a pouring temperature (TP) of 850 °C and stirring duration (SD) of 20 minutes which could be denoted as BP_4-CA_2-SP_4-TP_4-SD_4.

3.9. Estimating the Optimal Specific Wear Resistance

Based on the best combination of optimal levels of factors, the predicted optimum specific wear rate for the aluminum hybrid composites was 2.4002 x 10^{-6} mm^3/Nm.

3.10. Confirmation test

The confirmation test result of the specific wear rate is shown in Table 7 . From the table, an average specific wear rate of 2.5 x10^{-6} mm^3/Nm was obtained.

Table 8 compares predicted and experimental specific wear rates for the optimal processing conditions (A_4-B_2-C_4-D_4-E_4) of the hybrid aluminum matrix composite, including percentage error. From the analysis, a 3.992% experimental error was observed.

Figure 11(a) and (b) showcase the scanning electron microscopy (SEM) results of the optimal and control samples, respectively. From the figure the grey color portion represent the aluminum alloy, whereas the white dendrites and the dark color portion represent the Si-eutectoid phases along with brown pumice and coal respectively as posited by Mourad et al. (2023). The optimal sample exhibits a notably finer grain structure and fairly uniform distribution of the reinforcements in the aluminum matrix as shown in Figure 12 (b) compared to the control in the figure 12(b) which contributes to its higher wear resistance.

3.11. Optimal Sample Worn Surface Analysis

The wear tracks of the optimal sample undergo microstructure study to analyze the wear mechanism during tribological testing. Wear tracks of the samples are depicted in Figures 12. The SEM micrographs reveal that the worn surface is mainly characterized by longitudinal grooves (which are parallel to the sliding direction) and partially irregular pits, that indicate the presence of micro-cutting and micro-ploughing effect, suggesting domination of abrasive wear. Additionally, the micrographs also display the presence of pits and prows, indicating the occurrence of adhesive wear. Therefore, the overall microstructure study concludes that abrasive wear has primarily taken place, with some evidence of adhesive wear.

3.12. Regression analysis (modeling)

Table 9 shows that, at a 95% confidence level, only coal ash particulates and interaction within the coal ash particulates (CA^2) were insignificant on the specific wear rate of the produced hybrid aluminum composite with p-values above 0.05.

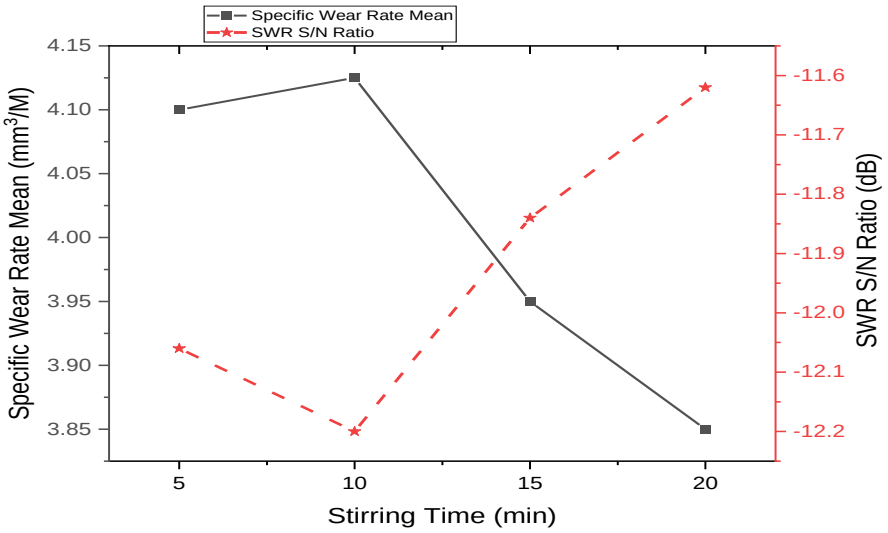

Figure 10. Variation of Stirring Durationwith Specific Wear Rate of the Aluminum Hybrid Composite.

Table 7. Specific Wear Rate Results for the Confirmation Test

Runs	Factors					Specific Wear Rate x 10^{-6}(mm³/Nm)			
(S/N)	BP (wt%)	CA (wt%)	SP (rpm)	TP (°C)	SD (min)	1	2	3	Average
1	10	5	500	850	20	2.3	2.5	2.6	2.5

Table 8. Predicted and Experimental

	Optimal process parameter settings	Predicted	Experimental	% Error
S/N ratio (dB)	BP_4-CA_2-SP_4-TP_4-SD_4	-7.60495	-7.959	4.446
SWR x 10^{-6} (mm³/m)		2.4002	2.5	3.992

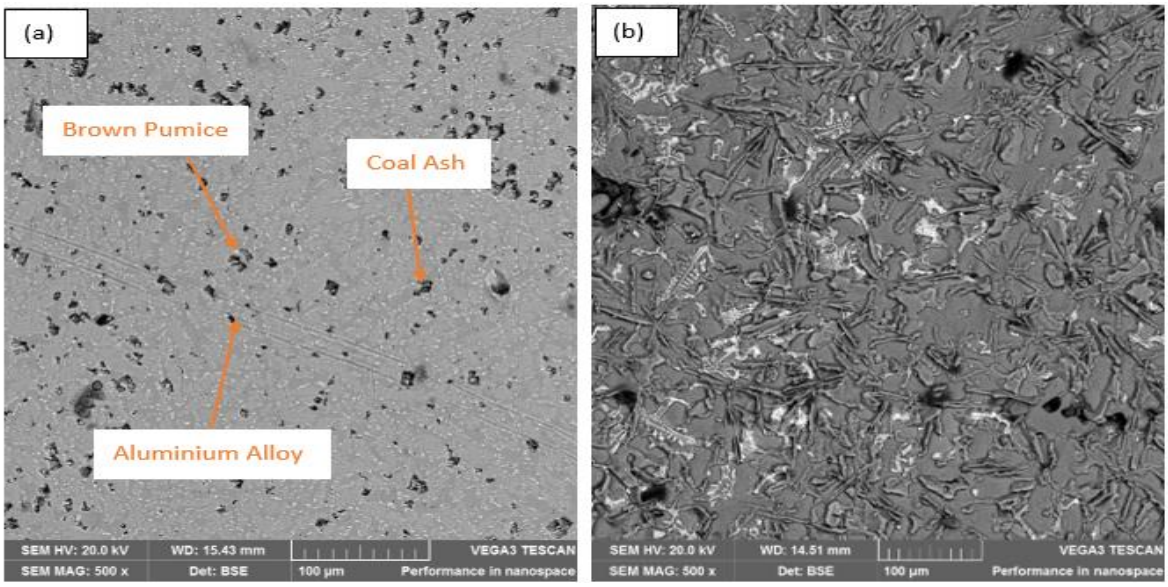

Figure 11. SEM Images of the (a) optimal and (b) Control

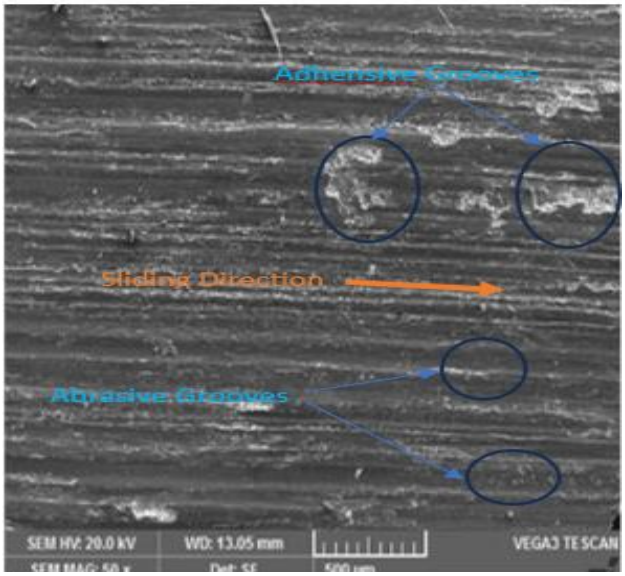

Figure 12. SEM Worn-out Track Surface of the Optimal Sample

Table 9. Analysis of Variance of Specific Wear Rate for the Hybrid Composite

Source	DF	Adj SS	Adj MS	F-Value	P-Value	% Contribution
Regression	8	6.7855	0.84819	26.52	0	
BP	1	2.7564	2.75637	86.2	0	47.57
CA	1	0.1657	0.16571	5.18	0.057	2.86
SP	1	0.2369	0.2369	7.41	0.03	4.09
TP	1	0.5951	0.59513	18.61	0.004	10.27
SD	1	0.2526	0.2526	7.9	0.026	4.36
CA*CA	1	0.9506	0.95062	29.73	0.001	16.4
SP*SP	1	0.133	0.13304	4.16	0.081	2.3
CA*SD	1	0.4807	0.48065	15.03	0.006	8.3
Error	7	0.2238	0.03198			3.86
Total	**15**	**5.7948**				**100**

From the regression analysis, a model for predicting the specific wear rate was derived and is shown by Equation 4.

$$\begin{aligned} SWR \times 10^{-6} = {} & 9.476 - 0.1613BP \\ & - 0.228CA - 0.00949SP \\ & - 0.003450TP \\ & + 0.0637SD \\ & + 0.03900CA^2 \\ & + 0.000010SP^2 \\ & - 0.01315CAxSD \end{aligned} \quad (4)$$

The model exhibited a high level of prediction accuracy for the specific wear rate of the aluminum composite, with R-Square, adjusted R-Square, and predicted R-Square values of 96.81%, 93.16%, and 80.74%, respectively. It is worth noting that the model used in the study demonstrated a remarkably high level of accuracy in predicting the specific wear rate of the aluminum composite. The R-Square, R-Square (adjusted), and R-Square (predicted) values were recorded at 96.81%, 93.16%, and 80.74%, respectively.

As per the studies conducted by Dan-Asabe *et al.* [21] and Sivaiahand Chakradh [52], an R-Square value greater than 75% is generally deemed acceptable, indicating a satisfactory fit between the process parameters and the responses. Figure 13illustrates curves of the specific wear rate data generated using the model equation (Equation 4) and the experimental values for the 16 different runs.

3.13. Confidence interval (CI)

A confidence interval value of ± 1.0869 was evaluated using Equation 3.7.The experimental specific wear rate (2.5 mm^3/Nm) obtained from the confirmatory test falls within the confidence interval range of the specific wear rate, confirming the validity of the experimental result within the confidence interval of 95%, as illustrated below:

$SWR_{predictive} - CI < SWR_{experimental} < SWR_{predictive} + CI$

$1.3133 < SWR_{experimental} < 3.4871$

4. Conclusion

This research aimed to improve the specific wear rate of Al-BP-CA hybrid composites intended for brake disc usage. The reinforcements, aluminum alloy, and hybrid composites were successfully developed and characterized. The specific wear rates of the developed hybrid aluminum metal matrix composite were evaluated and optimized using the Taguchi optimization and statistical regression techniques. From the analysis, the following conclusions were drawn:

1. X-ray fluorescence (XRF) analysis confirmed aluminum (Al), silicon (Si), and magnesium (Mg) as the primary elements in the aluminum alloy (AA6061). Coal ash was rich in silicon (Si), aluminum (Al), iron (Fe), titanium (Ti), and calcium (Ca). At the same time, pumice particles contained significant amounts of silicon (Si), iron (Fe), aluminum (Al), calcium (Ca), potassium (K), and titanium (Ti).
2. X-ray diffraction (XRD) identified silica (SiO2) and iron (III) oxide (Fe2O3) as the main phases in both brown pumice (BP) and coal ash (CA), indicating their suitability for reinforcement in various metal matrices. Additionally, coal ash contained graphite (C), potentially enhancing wear properties.
3. Thermogravimetric analysis (TGA) revealed good thermal stability for all materials, with the aluminum alloy (as-cast), brown pumice, and coal ash withstanding temperatures of 264.08 °C, 724 °C, and 605.51 °C, respectively.
4. Taguchi optimization identified a combination of 10% brown pumice particulates, 5% carbonated coal particles, a stirrer speed of 500 rpm, a pouring temperature of 850 °C, and a stirring duration of 20 minutes as optimal for achieving the lowest specific wear rate.
5. Brown pumice particulates significantly influenced the material's surface properties, contributing approximately 47.57% to the overall wear performance.
6. Developed regression models demonstrated high predictive capability for the material's specific wear rate, with R-squared values of 96.81% (R-Square), 93.16% (Adjusted R-Square), and 80.74% (Predicted R-Square). These values indicate a strong correlation between the model and the experimental data.

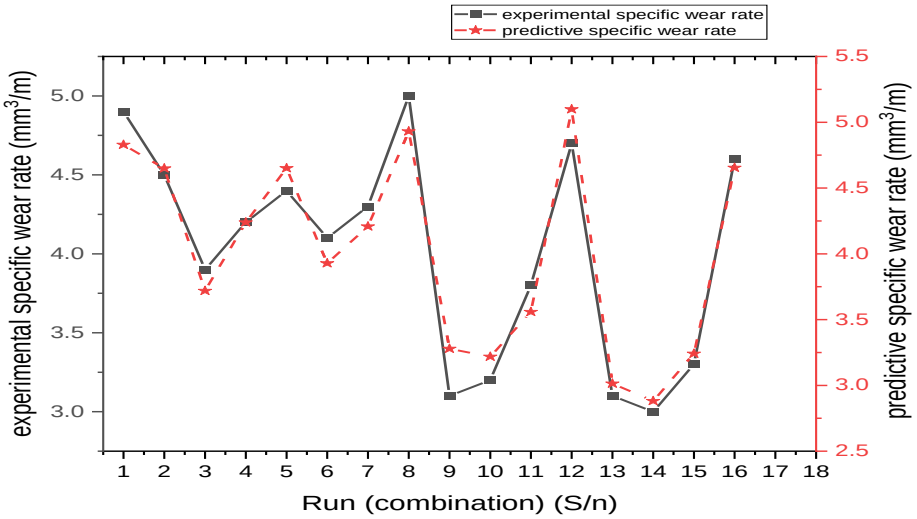

Figure 13. Experimental and Predictive Specific Wear Rate

Statements and Declarations

Funding

All authors certify that they have no affiliations with or involvement in any organization or entity with any financial interest or non-financial interest in the subject matter or materials discussed in this manuscript.

Competing Interests

The authors have no relevant financial or non-financial interests to disclose.

Author Contributions

Tanimu Kogi IBRAHIM: Conceptualization; Methodology; Investigation; Data curation; and Software.

Julius THADDAEUS: Methodology and Interpretation of Data

Popoola Caleb ABIODUN: Supervision; Conceptualization; Methodology; Validation; andWriting-Reviewing and Editing.

Ibrahim ILIYASU: Acquisition and analysis of Data; and Writing- Reviewing and Editing

Abdulmumin Akoredeley ALABI: Supervision; Writing- Reviewing and Editing

Data Availability

The raw/processed data required to reproduce these findings cannot be shared at this time as the data also forms part of an ongoing study (PhD Thesis).

References

[1] A. Adebisi, A. M. Md & Y. A. Mohammad "Wear Characteristics of Multiple Particle Size Silicon Carbide Reinforced Aluminium Composite", *Advanced Materials Research, 1115*, 2015, pp. 174-177.

[2] A. Adebisi, M. A Maleque, and M. B. Ndaliman, "Influence of Stirring Speed on Microstructure and Wear Morphology of SiCp-6061Al Composite", International Journal of Engineering Materials and Manufacture, Vol. 1, No. 1, 2016, pp. 21-26.

[3] A. Adebisi, M. B. Ndaliman, "Mathematical modelling of stir casting process parameters for AlSicp composite using central composite design", *28th AGM and International Conference of the Nigerian Institution for Mechanical Engineers*. Abuja: The Nigerian Institution for Mechanical Engineers, 2015.

[4] A. Adediran, K. K. Alaneme, I. O. Oladele, E. T. Akinlabi, "Wear characteristics of aluminum matrix composites reinforced with Si-based refractory compounds derived from rice husks" *Cogent Engineering, Vol*. 7 No. 1, 2020, p. 1826634.

[5] A. Victor and U. E. Inyang, "Development and Properties Characterization of Polyethylene Based Composite Using Coconut Fiber," JJMIE, vol. 81, no. 2, 2024.

[6] Abdelkawy, E. El-danaf and A. Almajid, "The Effect of Alloying, Processing and Heat Treatment on the Wear Resistance of Al-cu-mg-ag Alloys.," Jordan Journal of Mechanical & Industrial Engineering, vol. 17, no. 2, 2023.

[7] Apasi, P. B. Madakson, D. S. Yawas, and V. S. Aigbodion, "Wear Behaviour of Al-Si-Fe Alloy/Coconut Shell Ash Particulate Composites", *Tribology in Industry, Vol. 32, No.* 1, 2012, pp. 36-43.

[8] F. Abbas, A. E. Al-kawaz and Z. K. Mezaal, "Studying the Tribological and Mechanical Properties of the Pmma Nano Composite Coating," JJMIE, vol. 81, no. 2, 2024.

[9] Hajisadeghian, A. Masoumi, & A. Parvizi, "Investigation of the microstructure and thermo-mechanical properties of functionally graded materials fabricated by the vibrating centrifugal solid particle method". Proceedings of the Institution of Mechanical Engineers, Part B: *Journal of Engineering Manufacture, Vol. 236 No. 9,* 2022, pp. *1216-1231*.

[10] K. Azad, M. F. Saffiudeen, A. Syed and F. T. Mohammed, "Fabrication of Al-6061/sic Nano Composite Material through Ultrasonic Cavitation Technique and Its Analysis," JJMIE, vol. 17, no. 3, 2023.

[11] Kareem, J. A. Qudeiri, A. Abdudeen, T. Ahammed, & A. A Ziout, " Review on Aa 6061 Metal Matrix Composites Produced by Stir Casting", *Materials, Vol. 14 No.* 1, 2021, p, 175. https://doi:10.3390/ma14010175.

[12] Kheder, G. Marahleh and D. Al-jamea, "Strengthening of Aluminum by Sic, Al2o3 and Mgo.," Jordan Journal of Mechanical & Industrial Engineering, vol. 5, no. 6, 2011.

[13] Kumar-Sharma, R. Bhandar, A. Aherwar, R. Rimašauskiene, and C. Pinca-Bretotean, "A Study of Advancement in Application Opportunities of Aluminum Metal Matrix Composites", *Materials Today: Proceedings, Vol. 26, No.* 2, 2020, pp. 2419-2424.

[14] M. Razzaq, D. L. Majid, U. M. Basheer, & H. S. S. Aljibori, "Research Summary on the Processing, Mechanical and Tribological Properties of Aluminium Matrix Composites as Effected by Fly Ash Reinforcement" *Crystals, Vol. 11, No. 10,, 2021, p. 12*12.

[15] R. R. Kaladgi, K. F. Rehman, A. Afzal, M. A. Baig, M. E. M. Soudagar, & S. Bhattacharyya, "Fabrication characteristics and mechanical behavior of aluminium alloy reinforced with Al2O3 and coconut shell particles synthesized by stir casting", In IOP Conference Series: *Materials Science and Engineering Vol. 1057, No. 1,* 2021, *p. 012017. IOP Publishing*.

[16] Rahman, O. Adeboye, a. Adebayo and M. Salleh, "Behaviour and Some Properties of Wood Plastic Composite Made from Recycled Polypropylene and Rubberwood.," Jordan Journal of Mechanical & Industrial Engineering, vol. 17, no. 2, 2023.

[17] Rai, B. Mohanty, R. Bhargava, "Supercritical extraction of sunflower oil: a central composite design for extraction variables", *Food Chem., Vol. 192,* 2016, pp. 647–659.

[18] Sharma, N. Sakimoto, & T. Takanohashi, "Effect of binder amount on the development of coal-binder interface and its relationship with the strength of the carbonised coal-binder composite", *Carbon Resources Conversion,* Vol. *1, No.* 2, 2018, pp. 139-146.

[19] Advesh, "Development and property evaluation of aluminum alloy reinforced with nano-zro2 metal matrix composites (nmmcs) for automotive applications", *Doctor of Philosophy Thesis*. Dr. MGR Educational and Research Institute, Deemed University), Department of Mechanical, Maduravoyal, Chennai, 2011.

[20] Bachchhav and K. Hendre, "Wear Performance of Asbestos-free Brake Pad Materials.," Jordan Journal of Mechanical & Industrial Engineering, vol. 16, no. 4, 2022.

[21] Dan-Asabe, S. A. Yaro, D. S. Yawas, & S. Y. Aku, "Statistical modeling and optimization of the flexural strength, water absorption and density of a doum palm-Kankara clay filler hybrid composite", *Journal of King Saud University-Engineering Sciences*, Vol. *31, No.* 4, 2019, pp. 385-394.

[22] M. Gowda, R. Joshi, and R Kuntanahal, "Studies on Bottom Ash Strengthened LM13 Composite", *Materials Today: Proceedings, 20,* 2020, 217-221. https://doi:10.1016/j.matpr.2019.11.119.

[23] Vinod, S. Ramanathan, V. Ananthi, & N. Selvakumar, "Fabrication and characterisation of organic and in-organic

reinforced A356 aluminium matrix hybrid composite by improved double-stir casting". *Silicon*, Vol *11, No.* 2, 2019, pp. 817–829.

[24] B., Ersoy, A. Sariisik, S. Dikmen, & G. Sariisik, "Characterization of Acidic Pumice and Determination of its Electrokinetic Properties in Water", *Powder Technology, Vol. 197*, 2010, pp. 129–135. https://doi:10.1016/j.powtec.2009.09.005.

[25] Ekpruke, C. Ossia and a. Big-alabo, "On the Morphological and Tribological Characterization of Green Automotive Brake Pads Developed from Waste Thais Coronata Seashells.," Jordan Journal of Mechanical & Industrial Engineering, vol. 17, no. 2, 2023.

[26] Cilento, A. Martone, M. G. P. Carbone, C. Galiotis,, & M. Giordano, "Nacre-like GNP/Epoxy composites: Reinforcement efficiency vis-a-vis graphene content". *Composites Science and Technology, Vol. 211*, 2021, p. *108873*.

[27] Dixit and M. M. Khan, "Sliding Wear Response of an Aluminium Metal Matrix Composite: Effect of Solid Lubricant Particle Size.," Jordan Journal of Mechanical & Industrial Engineering, vol. 8, no. 6, 2014.

[28] Guo, S. Li, Z. Yang, X. Su, S. Zhao, B. Song, & S. Shi, "Effect of continuous micro-aeration on hydrogen production by coal bio-fermentation", *Energy Sources, Part A: Recovery, Utilization, and Environmental Effects*, 2022, *pp. 1-11*.

[29] Hanizam, M. S. Salleh, M. Z. Omar, & A. B. Sulon, "Optimisation of mechanical stir casting parameters for fabrication of carbon nanotubes–aluminium alloy composite through Taguchi method" *Journal of Materials Research and Technology*, Vol. *8* No. 2, 2019, pp. 2223-223.

[30] Sun, Y. Zhao, S. Jiao, C. Wang, Y. Jia,, K. Dai, ... & C. Shen, "Environment tolerant conductive nanocomposite organohydrogels as flexible strain sensors and power sources for sustainable electronics", *Advanced Functional Materials*, Vol. 31, No. 24, 2021, p. 2101696.

[31] M. Ersoy a, & K. K. Adama, "Property evaluation of pumice particulate-reinforcement in recycled beverage cans for Al-MMCs manufacture", *Journal of King Saud University-Engineering Sciences*, Vol. *3, No.* 1, 2018, pp. 61-67.

[32] İ. Pınarcı, & Y. Kocak, "Hydration mechanisms and mechanical properties of pumice substituted cementitious binder", *Construction and Building Materials*, Vol. *335*, 2022, p. 127528.

[33] Hashim, L. Looney, & M. S. J. Hashmi, "The Wettability of SiC Particles by Molten Aluminium Alloy", *Journal of Materials Processing Technology, Vol. 119*, 2001, pp. 324-32.

[34] J. K. Abifarin, D. O. , Olubiyi, E. T. Dauda, Oyedeji, E. O, "Taguchi Grey Relational Optimization of the Multi-mechanical Characteristics of Kaolin Reinforced Hydroxyapatite: Effect of Fabrication Parameters", *International Journal of Grey Systems*, Vol. *1, No.* 2, 2021, pp. 20–32.

[35] Aithal, B. N. Ramesh, H. Manjunath and K. Chethan, "Characterization of Al-sicp Functionally Graded Metal Matrix Composites Developed through Centrifuge Casting Technique," JJMIE, vol. 15, no. 5, 2021.

[36] K. G. Satyanarayana, R. M. Pillai, & B. C. Pai, "Aluminum cast metal matrix composite. In Handbook of ceramics and composites, CRC Press ; 2021, pp. 555-599..

[37] Sivaraos, K. Milkey, A. Samsudin, A. Dubey and P. Kidd, "Comparison between Taguchi Method and Response Surface Methodology (RSM) in Modelling Co 2 Laser Machining.," Jordan Journal of Mechanical & Industrial Engineering, vol. 8, no. 1, 2014.

[38] K. Sadashiva and K. Purushothama, "Investigation on Mechanical and Morphological Characteristics of Ramie/silk with Epoxy Hybrid Composite of Filler Ommt Nanoclay.," Jordan Journal of Mechanical & Industrial Engineering, vol. 17, no. 2, 2023.

[39] C. Aguilar Esteva, A. Kasliwal, M. S. Kinzler, H. C. Kim, & G. A. Keoleian, "Circular economy framework for automobiles: Closing energy and material loops', *Journal of Industrial Ecology*, Vol. 25, No. 4, 2021, pp. 877-889.

[40] N. Abijith, A. R. Nair, M. Aadharsh, R. V. Vignesh, R. Padmanaban and M. Arivarasu, "Investigations on the Mechanical, Wear and Corrosion Properties of Cold Metal Transfer Welded and Friction Stir Welded Aluminium Alloy Aa2219.," Jordan Journal of Mechanical & Industrial Engineering, vol. 12, no. 4, 2018.

[41] M. Ali and S. Falih, "Synthesis and Characterization of Aluminum Composites Materials Reinforced with Tic Nano-particles.," Jordan Journal of Mechanical & Industrial Engineering, vol. 8, no. 5, 2014.

[42] M. Hassan, & V. G. Gomes, "Coal derived carbon nanomaterials–Recent advances in synthesis and applications", *Applied Materials Today*, Vol. *12*, 2018, pp. 342-358.

[43] M. K. Gupta, M. Ramesh, & S. Thomas, "Effect of hybridization on properties of natural and synthetic fiber-reinforced polymer composites (2001–2020): A review" *Polymer Composites, Vol. 42, No. 10*, 2021, pp. *4981-5010*.

[44] M. Kok, "Production and Mechanical Properties of Al_2O_3 Particle-Reinforced 2024 Aluminium Alloy Composites", *Journal of Materials Processing Technology, Vol. 161*, 2005, pp. 381–387.

[45] M. Nodehi, "A comparative review on foam-based versus lightweight aggregate-based alkali-activated materials and geopolymer", Innovative Infrastructure Solutions, Vol. 6, No. 4, 2021, 1-20.

[46] M. R. A. Karim, S. A. Raza, M. I. Khan, A. B. Tahir, E. U. Haq, & M. Pavese, "Electrodeposition of nickel–graphene nanoplatelets (GNPs) composite coatings and evaluation of their morphological, electrochemical, and thermo-mechanical properties". Applied Physics A, Vol. 128 , No. 6, 2022, pp. 1-13.

[47] Gencel, "Characteristics of Fired Clay Bricks with Pumice Additive", *Energy and Buildings, Vol. 102*, 2015, pp. 217-224. https://doi:10.1016/j.enbuild.2015.05.03.

[48] P, I. Peter, & A, A. Adekunle, "A review of ceramic/bio-based hybrid reinforced aluminum matrix composites", *Cogent Engineering*, Vol *7, No.* 1, 2020, p. 1727167.

[49] Jayakrishnan, & M. T. Ramesan, "Synthesis, characterisation and properties of poly (vinyl alcohol)/chemically modified and unmodified pumice composites", *Journal of Chemical and Pharmaceutical Sciences ISSN*, Vol. *974*, 2016, p. 2115.

[50] K. Jayashree, M. C. G. Shankar, A. Kini, S. S. Sharma, & R. Shetty, "Review on Effect of Silicon Carbide (SiC) on Stir Cast Aluminium Metal Matrix Composites", *International Journal of Current Engineering and Technology, Vol. 3, No.* 3, 2013, pp. 1061-1071.

[51] P. P. Ikubanni, M. Oki, A. A. Adeleke, & P. O. Omoniyi, "Synthesis, Physico-mechanical and Microstructural Characterization of Al6063/sic/pksa Hybrid Reinforced Composites". *Scientific Reports, 11*(1) 2021. http://doi:10.1038/s41598-021-94420-0

[52] P. Sivaiah, & D. Chakradhar, "Modeling and optimization of sustainable manufacturing process in machining of 17-4 PH stainless steel. Measurement", *Measurement 134*, 2019, pp. 142–152

[53] Ashok-Kumar, and A. Devaraju, "Modeling of Mechanical Properties and High Temperature Wear Behavior of Al7075/SiC/CRS Composite Using RSM", *Silicon 13*, 2021, pp. 3499–3519. https://doi:10.1007/s12633-020-00801-x.

[54] Gupta, S. Sharma, T. Nanda, and O. P. Pandey, "Wear Studies of Hybrid AMCs Reinforced with Naturally Occurring Sillimanite and Rutile Ceramic Particles for Brake-Rotor

Applications", *Ceramics International, Part B, Vol. 46*, No. 10, 2020, pp. 16849-16859. https://doi:10.1016/j.ceramint.2020.03.262.

[55] R. Manjunath, D. Kumar, & A. A. Kumar, "Review on the significance of hybrid particulate reinforcements on the mechanical and tribological properties of stir-casted aluminum metal matrix composites. Journal of Bio-and Tribo-Corrosion", Vol. 7, No. 3, 2021, pp. 1-11.

[56] R. R. Veeravalli, R. Nallu, and M. M. Mohiuddin-S, "Mechanical and tribological properties of AA7075–TiC metal matrix composites under heat treated (T6) and cast conditions", *Journal of Materials Research and Technology,, Vol. 5*, No. 4, 2016,pp. 377–383. doi:10.1016/j.jmrt.2016.03.011.

[57] A. Rizvi and S. Tewari, "Optimization of Welding Parameters by Using Taguchi Method and Study of Fracture Mode Characterization of Ss304h Welded by Gma Welding.," Jordan Journal of Mechanical & Industrial Engineering, vol. 12, no. 1, 2018.

[58] S. B. Prabu,L. Karunamoorthy, S. Kathiresan, B. Mohan, "Influence of stirring speed and stirring time on distribution of particles in cast metal matrix composite", *Journal of Materials Processing Technology*, Vol. *171, No.* 2, 2006, pp. 268-273.

[59] S. Channappagoudar, K. Aithal, N. Sannayallappa, V. Desai and P. G. Mukunda, "The Influence of the Addition of 4.5 Wt.% of Copper on Wear Properties of Al-12si Eutectic Alloy," Jordan Journal of Mechanical and Industrial Engineering, vol. 9, no. 3, 2015.

[60] S. Dayanand, S. B., Boppana, V. Auradi, M. Nagaral, & M. Udaya Ravi, "Evaluation of Wear Properties of Heat-Treated Al-AlB2 In-Situ Metal Matrix Composites", *Journal of Bio- and Tribo-Corrosion, Vol. 7, No, 2,* 2021, *pp. 1-11*.

[61] S. G. Ghalme, "Improving Mechanical Properties of Rice Husk and Straw Fiber Reinforced Polymer Composite through Reinforcement Optimization.," Jordan Journal of Mechanical & Industrial Engineering, vol. 15, no. 5, 2021.

[62] S. N. Prashant, M. Nagaral, & V. Auradi, "Preparation and Evaluation of Mechanical and Wear Properties of Al6061 Reinforced with Graphite and SiC Particulate Metal Matrix Composites", *International Journal of Engineering and Robotic Research, Vol. 1,* No. 3, 2012, pp. 106-112.

[63] S. Sarkara, R. Mandala, N. Mondalb, S. Chaudhuric, T. Mandald and G. Majumdara, "Modelling and Prediction of Micro-hardness of Electroless Ni-p Coatings Using Response Surface Methodology and Fuzzy Logic," Jordan Journal of Mechanical and Industrial Engineering, vol. 16, no. 5, 2022.

[64] S. Verma, V. Kakkar, & H. Singh, "Optimisation of Cutting Forces in Dry Turning Process Using Taguchi and Grey Relational Analysis", In *Recent Advances in Operations Management Applications*, 2022, pp. 317-334

[65] S. Wakeel, S. Bingol, M. N. Bashir, & S. Ahmad, "Selection of sustainable material for the manufacturing of complex automotive products using a new hybrid Goal Programming Model for Best Worst Method–Proximity Indexed Value method", Proceedings of the Institution of Mechanical Engineers, Part L: *Journal of Materials: Design and Applications, Vol. 235, No. 2, 2021, pp. 385-399.*

[66] V.Sadi, M. W.Malau, Wildan, & Suyitno, "Optimization of Stir Casting Process Parameters to Minimize the Specific Wear of Al-SiC Composites by Taguchi Method", *International Journal of Engineering and Technology, Vol.7, No.* 1, 2015, pp. 17-26.

[67] Alsardia and L. Lovas, "Investigation of the Effect of the Surface Treatment and Lubrication during Repeated Tightening on the Nut Coefficient of a Bolted Joint Using the Taguchi Method," JJMIE, vol. 81, no. 1, 2024.

[68] T. K. Ibrahim, I. Iliyasu and P. C. Abiodun, "Application of Taguchi Methods and Regression Analysis to Optimize Process Parameters and Reinforcements for Maximizing Composite's Coefficient of Friction for Brake Disc Application: a Statistical Optimization Approach," *Journal of Sustainable Materials Processing and Management*, Vol. 4, no. 1, pp. 89-105, 2024.

[69] T. Ibrahim, D. S. Yawas, & S. Y. Aku, "Effects of Gas Metal Arc Welding Techniques on the Mechanical Properties of Duplex Stainless Steel". *Journal of Minerals and Materials Characterization and Engineering, Vol. 1,* 2013, pp. *222-230.*

[70] T. K. Ibrahim, D. S. Yawas, B. Dan-asabe, & A. A. Adebisi"Manufacturing and Optimization of the Effect of Casting Process Parameters on the Compressive Strength of Aluminum/Pumice/Carbonated Coal Hybrid Composites: Taguchi And Regression Analysis Approach", *International Journal of Advance Manufacturing*, vol. 125, 2023, pp. 3401–3414. https://doi:10.1007/s00170-023-10923-2.

[71] T. K. Ibrahim, D. S. Yawas, B. Dan-asabe, & A. A. Adebisi, "Optimization and statistical modeling of the thermal conductivity of a pumice powder and carbonated coal particle hybrid reinforced aluminum metal matrix composite for brake disc application: a Taguchi approach", Functional *composite and structure Vol. 5, No. 1,* 2023, p. *015008*. https://doi.org/10.1088/2631-6331/acc0d1.

[72] T. K. Ibrahim, D. S. Yawas, B. Dan-asabe, & A. A. Adebisi, "Taguchi optimization and modelling of stir casting process parameters on the percentage elongation of aluminium, pumice and carbonated coal composite", *Scientific Report, Vol. 13*, 2023, 2915. https://doi:10.1038/s41598-023-29839-8.

[73] T. K. Ibrahim, D. S. Yawas, J. Thaddaeus, B. Danasabe, I. Iliyasu, A. A. Adebisi and T. O. Ahmadu, "Development, Modelling and Optimization of Process Parameters on the Tensile Strength of Aluminum, Reinforced with Pumice and Carbonated Coal Hybrid Composites for Brake Disc Application," Scientific Reports, vol. 14, no. 1, p. 16999, 2024.

[74] T. Tran and V. H. Dai, "Multi-objective Optimization of CNC Milling Parameters of 7075 Aluminium Alloy Using Response Surface Methodology," JJMIE, vol. 17, no. 3, 2023.

[75] K. Vasu and U. Ks, "Empirical Analysis of Multiwalled Carbon Nanotube Deposition for Enhancing Mechanical and Tribological Characteristics in Aluminium-based Metal Matrix Composites.," Jordan Journal of Mechanical & Industrial Engineering, vol. 17, no. 4, 2023.

[76] Malau, M. W. Wildan, Suyitno and Sadi, "Optimization of Process Parameters of Stir Casting to Maximize the Hardness of Al-SiC Composites by Taguchi Method", *International Journal of Applied Engineering Research,Vol. 9 No.* 24, 2014, pp. 30121-30134.

[77] V. R. Rao, N. Ramanaiah and M. Sarcar, "Optimization of Volumetric Wear Rate of Aa7075-tic Metal Matrix Composite by Using Taguchi Technique.," Jordan Journal of Mechanical & Industrial Engineering, vol. 10, no. 3, 2016.

[78] V. S. Aigbodion, "Development of Al-Si-Fe/Rice Husk Ash Particulate Composites Synthesis by Double Stir Casting Method", *Usak University Journal of Material Sciences, Vol. 2*, 2012, pp. 187 – 197.

[79] V. Sahajwalla, M. Zaharia, I. Mansuri, R. Rajarao, R. Dhunna,, F. Nur Yunos, R. Khanna, "The Power of Steelmaking — Harnessing High-Temperature Reactions to Transform Waste into Raw Material Resources", *Association of Iron Steel and Technology, 2013*, pp. 1-16.

[80] V.S. Aigbodion, & S. B, Hassan, "Experimental correlations between wear rate and wear parameter of Al–Cu–Mg/bagasse ash particulate composite", *Journal of Materials & Design, Vol. 31 No.* 4, 2010, pp. 2177–2180. https://doi:10.1016/j.matdes.2009.10.055.

[81] Yang, H. Zhang, P. Dong, Z. Yan, & W. Wang, "A study on the formation of multiple intermetallic compounds of friction stir processed high entropy alloy particles reinforced Al matrix

composites", *Materials Characterization*, Vol. 183, 2022, p. 111646.

[82] Liu, L. He and S. Yuan, "Wear Properties of Aluminum Alloy 211z. 1 Drilling Tool.," Jordan Journal of Mechanical & Industrial Engineering, vol. 15, no. 1, 2021.

[83] Peng, Y. Liu, B. Zhan, & G Xu, "Preparation of autoclaved aerated concrete by using graphite tailings as an alternative silica source", Construction and Building Materials, Vol. 267, 2021, p. 121792.

[84] Y. Sinshaw,, B. Sirahbizu-Y., S. Palani, and U. Prakash-J, "Mechanical Property Analysis of Glass Particulates Reinforced Aluminum Matrix Composites". *Materials Today: Proceedings, Vol. 62, No. 17, 2022, 488-494*. https://doi.org/10.1016/j.matpr.2022.03.572.

[85] Tan, J. Li, & Z. Zhang, "Experimental and numerical studies on fabrication of nanoparticle reinforced aluminum matrix composites by friction stir additive manufacturing". *Journal of Materials Research and Technology, Vol. 12, 2021, pp. 1898-1912*.

[86] T. Ibrahim, D. S. Yawas, & S. Y. Aku,"Effects of Shield Metal Arc Welding Techniques on the Mechanical Properties of Duplex Stainless Steel"*Journal of Advance in Applied Science Research, Pelagia Research Library*vol. *4, no. 50, 2013, 190-201*.

[87] R. A. Kumar, B. I. Prasad, C. Bibin, I. J. Thomas, G. Soundararajan, P. Darshan and S. Arunkumar, "Physical and Mechanical Characterization of Al7075/si3n4 Metal Matrix Composite Prepared by Stir Casting Technique," *Materials Today: Proceedings,* vol. 80, 2023 pp. 176-182.